Volume 48 | Number 46 | 14 December 2019 | Pages 17135–17424

Dalton Transactions

An international journal of inorganic chemistry

rsc.li/dalton

ISSN 1477-9226

ROYAL SOCIETY OF CHEMISTRY | Celebrating IYPT 2019

COMMUNICATION

Artur Kasprzak and Hidehiro Sakurai

Site-selective cation–π interaction as a way of selective recognition of the caesium cation using sumanene-functionalized ferrocenes

Dalton Transactions

COMMUNICATION

Cite this: *Dalton Trans.*, 2019, **48**, 17147

Received 3rd August 2019,
Accepted 23rd September 2019

DOI: 10.1039/c9dt03162f

rsc.li/dalton

Site-selective cation–π interaction as a way of selective recognition of the caesium cation using sumanene-functionalized ferrocenes†

Artur Kasprzak *[a] and Hidehiro Sakurai [b]

The first sumanene–ferrocene probes for efficient and selective caesium cation (Cs^+) recognition are reported. The working mechanism of the sumanene moiety as the sensing unit was based on the site-selective cation–π interaction in its neutral state. The interactions with Cs^+ were characterized by high association constant values together with low limits of detection.

The design of selective caesium cation (Cs^+) sensors constitutes a great challenge and is of the highest environmental importance in the modern world, because of the presence of this cation in nuclear plant waste coming from the reprocessing of irradiated fuels.[1] Several classes of organic compounds have been reported as Cs^+ recognition materials, most commonly fluorescent probes based on calixarene-templated crown ethers.[2] The working mechanism of these types of sensors was based on the size-selective recognition and the formation of a complex between the crown ether unit and Cs^+ through the ion–dipole electrostatic interaction. These compounds exhibited superior properties toward Cs^+ recognition compared to the other metal cations, such as Na^+, Mg^{2+} or Rb^+.

Electrochemical probes can be applied for the real-time detection of various analytes, including pollutants, such as metal ions, because of the sensitivity, selectivity, portability and fast analytical response time of such sensors.[3] The use of ferrocene (Fc) in the construction of ion sensors is of general interest.[4] Fc-based electrochemical probes show reversible and quantitative reduction–oxidation behaviour, associated with the presence of the ferrocene/ferrocenium (Fc/Fc^+) redox couple. The ion recognition phenomenon can be easily tracked by various electrochemical methods, such as the commonly used cyclic voltammetry (CV) technique. Upon addition of an ion, a change in the Fc's oxidation/reduction potential position is commonly observed.[5] All of the mentioned features make Fc derivatives ideal candidates for ion recognition materials.

Sumanene (**1**) is a bowl-shaped molecule belonging to the class of so-called buckybowls (Fig. 1a).[6] Due to its interesting physicochemical properties, the chemistry of sumanene has been intensively studied since its first synthesis in 2003.[7] The reports covered for example the creation of sumanene-based supramolecular architectures[8] and self-assembly studies with sumanenylferrocenes.[9]

In 2017, the collaborative effort of Hirao, Petrukhina and Rogachev groups resulted in the preparation of a novel organometallic sumanene-based compound of Cs^+.[10] The driving force for the formation of such a unique sandwich complex (Fig. 1b) is a perfect match of Cs^+ with the sumanene's concave cavity. The caesium cation was encapsulated by two sumanenyl monoanions, generated by the reaction of sumanene with sodium as a solvent-separated ion pair. Encouraged by this report, in pursuit of the design of new selective and efficient Cs^+ sensors, we envisaged that ferrocene–sumanene conjugates may act as caesium cation recognition materials. To our surprise, the sumanene moiety was found to work as a sensing unit even in the neutral state only through the cation–π interaction. Presented herein is our detailed research on the synthesis and the metal cation binding of novel conjugates of ferrocene and sumanene.

The synthetic design involved the conjugation of formylsumanene (**2**) and aminosumanene (**7**) with ferrocene (Fc) derivatives bearing either the primary amine group (in the case of

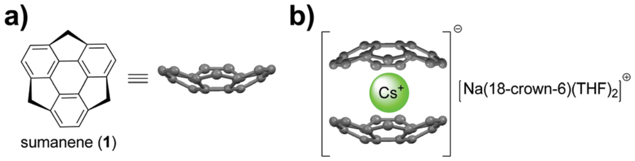

Fig. 1 (a) Structure of sumanene (**1**) and (b) structure of the reported example of the $Cs^+(sumanene)_2$-type sandwich complex.[10]

---

[a] *Faculty of Chemistry, Warsaw University of Technology, Noakowskiego Str. 3, 00-664 Warsaw, Poland. E-mail: akasprzak@ch.pw.edu.pl*
[b] *Division of Applied Chemistry Graduate School of Engineering, Osaka University, 2-1 Yamadaoka, Suita, Osaka 565-0871, Japan*

† Electronic supplementary information (ESI) available: Experimental section, characterization data, and metal binding experiments. See DOI: 10.1039/C9DT03162F

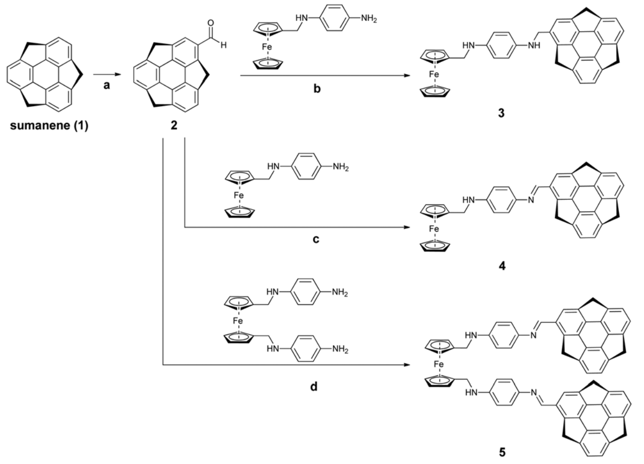

Scheme 1 Synthesis of ferrocenyl derivatives of sumanene **3–5**: (a) see ref. 12; (b) *N*-(ferrocenylmethyl)benzene-1,4-diamine 100 mol% in MeOH, formylsumanene 100 mol% in THF, formic acid (cat.), 27 °C, 24 h, then $NaBH_4$ 300 mol%, 27 °C, 3 h, 75% yield; (c) *N*-(ferrocenylmethyl) benzene-1,4-diamine 100 mol% in MeOH, formylsumanene 100 mol% in THF, formic acid (cat.), 27 °C, 24 h, 94% yield; (d) N^1,N^1-(1,1′-bis(methyl) ferrocenyl)bis(benzene-1,4-diamine) 100 mol% in MeOH, formylsumanene 200 mol% in THF, formic acid (cat.), 27 °C, 24 h, 72% yield.

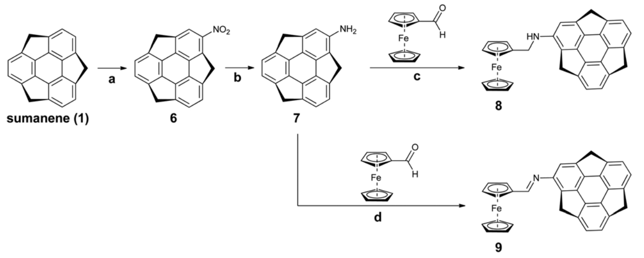

Scheme 2 Synthesis of ferrocenyl derivatives of sumanene **8–9**: (a) see ref. 12; (b) nitrosumanene 100 mol%, Pd/C 200 wt%, H_2, EtOH/AcOEt, 27 °C, 3 h, 99% yield; (c) formylferrocene 100 mol%, aminosumanene 100 mol%, formic acid (cat.), MeOH, reflux 6 h, then $NaBH_4$ 300 mol%, reflux, 1 h, 69% yield; (d) formylferrocene 100 mol%, aminosumanene 100 mol%, formic acid (cat.), MeOH, reflux 6 h, 61% yield.

sumanene derivative **2**; Scheme 1) or the formyl functionality (in the case of sumanene derivative **7**; Scheme 2).[11] Both mono- and di-substituted Fc derivatives were included in our studies. In brief, formylsumanene (**2**) was prepared by the aromatic electrophilic substitution reaction using sumanene (**1**) as the starting material (Scheme 1a), whilst aminosumanene (**7**) was prepared by the Pd-catalysed hydrogenation reaction starting from nitrosumanene (**6**) (Scheme 2a and b). Ferrocene–sumanene conjugates were obtained in good yields by means of the reductive amination reaction (compounds **3** and **8**; Schemes 1b and 2c), or condensation for imine formation (compounds **4**, **5** and **9**; Schemes 1c, d and 2d). As a result, various mono- or di-substituted ferrocenyl derivatives of sumanene were prepared, with the difference in the type of linkage between these motifs, *i.e.*, compounds containing a *p*-phenylenediamine-type spacer (**3–5**) or linked directly (**8–9**) and compounds containing a CH_2NH-type (**3**, **8**) or an imine-type (**4**, **5**, and **9**) linker.

Formation of the desired products was confirmed spectroscopically (NMR, IR, UV-Vis, and MS). ^1H NMR spectra showed the characteristic peaks coming from both structural moieties, *i.e.* ferrocene (H of cyclopentadienyl (Cp) rings) and sumanene (H_{Ar}, benzylic H_{endo} and H_{exo}), as well from the introduced linkers, including the imine peak at *ca.* 8.60–8.55 ppm for compounds **4**, **5**, and **9**.[13] The structural elucidation of **3**, **4** and **5** was also supported by 2-D NMR experiments (^1H–^1H COSY and ^1H–^1H TOCSY).[14] The presence of the desired structural motifs in the obtained conjugates was also confirmed by IR spectroscopy, as the characteristic absorption bands coming from the Fc, (*e.g.*, 1520–1510 cm^{-1}) and the introduced linkages (*e.g.*, imine – 1660–1630 cm^{-1} and amine – 1560–1530 cm^{-1}) were observed.[15] The UV-Vis spectra of the obtained compounds consisted of the absorption maxima coming from the sumanene (*ca.* 280–250 nm) and ferrocene (*ca.* 390–360 nm) moieties.[16,17]

Cyclic voltammetry (CV) experiments revealed the reversible reduction–oxidation electrode process for all the ferrocene–sumanene conjugates, due to the presence of the Fc/Fc^+ redox couple. The electrochemical parameters of the studied Fc-sumanene conjugates are listed in Table 1. The peak position depended on the type of substituent on the Cp ring[18] and was found to be the highest for compound **9** (Fc-CH═N-sumanene; $E^{ox}_{1/2}$ = 0.751 V) and the lowest for compound **8** (Fc-CH_2NH-sumanene; $E^{ox}_{1/2}$ = 0.577 V).[19]

The thus-obtained ferrocene–sumanene conjugates were applied for the caesium cation (Cs^+) recognition. First, the interactions were studied by fluorescence spectroscopy. The titration experiment for Cs^+ and the representative conjugate **3** is presented in Fig. 2.[21,22] All the conjugates exhibited 'turn-off' fluorescence behaviour (lowering of the emission intensity) after the addition of further portions of Cs^+. Such a feature indicates the ion recognition phenomenon.[23] The continuous variation method (Job's plot method) revealed the 1 : 1 binding mode for the di-sumanenyl ferrocene derivative (**5**), whilst the 2 : 1 mode (conjugate : Cs^+) was found for the mono-sumanenyl ferrocenes.[24] Thus, the structures of the complexes were hypothesized (Fig. 3). The sandwich complexes are comprised of one caesium cation and (1) two Fc-templated sumanene molecules – compounds **3**, **4**, **8**, and **9** (Fig. 3a) or (2) one Fc-

Table 1 Data for the electrochemical parameters of the obtained Fc–sumanene conjugates[20]

Entry	Compound label	$E^{ox}_{1/2}$ [a] [V]	Electrode process
1	**3**	0.625	Reversible
2	**4**	0.621	Reversible
3	**5**	0.674	Reversible
4	**8**	0.577	Reversible
5	**9**	0.751	Reversible

[a] Conditions: CH_2Cl_2, 0.5 mM Fc–sumanene conjugate, 0.1 M tetra-*n*-butylammonium perchlorate (TBAP), scan rate; 0.05 V s^{-1}.

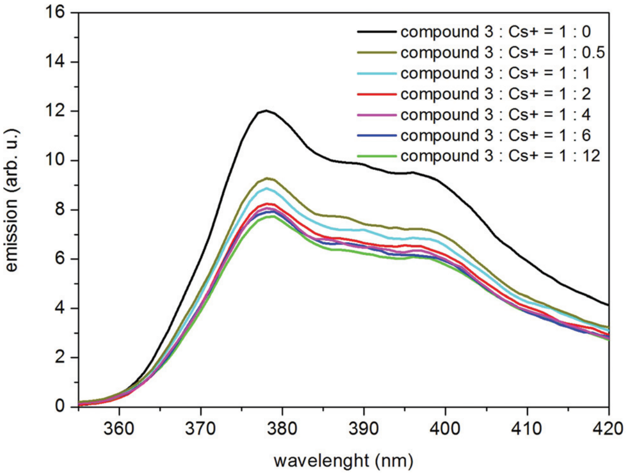

Fig. 2 Caesium (Cs^+) binding studies with compound **3** using the fluorescence spectra titration method (excitation wavelength: 280 nm).

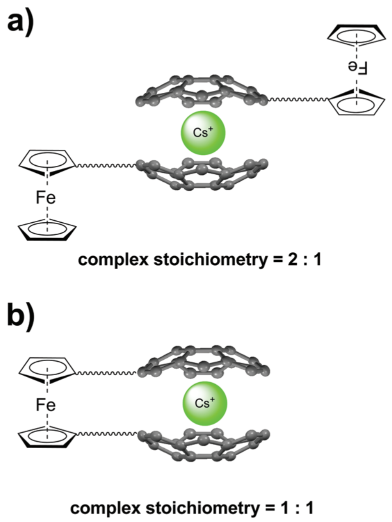

Fig. 3 Hypothetical structures of the studied complexes: (a) for compounds **3**, **4**, **8**, and **9** and (b) for compound **5**.

sumanene molecule 'wrapping' Cs^+ – compound **5** (Fig. 3b). It is noteworthy that the sumanene moiety remains neutral throughout the complexation, therefore the driving force for wrapping was the site-selective 'cation–π interaction' between the concave face of sumanene and Cs^+.[10,25]

The change in the emission intensity differed between the samples, as a result of different association constant values (K_a). The association constant values and the limits of detection (LOD) were calculated using the Stern–Volmer equation.[26] The data for compounds **3–5** and **8–9** are summarized in Table 2. It is noteworthy that the Stern–Volmer model is used to describe 1 : 1 systems, however, both the $I_0/I = f(C_{\text{cation}})$ and $I_0/I = f(C_{\text{cation}}^2)$ plots for compounds **3**, **4**, **8**, and **9** (2 : 1 complexes) were found to be linear. Nevertheless, the K_a values calculated for these systems should be treated as the approximate

Table 2 Caesium (Cs^+) binding parameters exhibited by the ferrocene–sumanene conjugates (**3–5** and **8–9**)

Entry	Compound label	K_a	LOD [M]
1	**3**	*ca.*[a] $4.5 \times 10^5\ M^{-2}$	1.8×10^{-5}
2	**4**	*ca.*[a] $4.9 \times 10^4\ M^{-2}$	7.0×10^{-5}
3	**5**	$8.9 \times 10^4\ M^{-1}$	1.2×10^{-5}
4	**8**	*ca.*[a] $2.9 \times 10^5\ M^{-2}$	1.5×10^{-5}
5	**9**	*ca.*[a] $1.7 \times 10^4\ M^{-2}$	3.8×10^{-5}

[a] 2 : 1 complex; the approximate K_a value was calculated based on the $I_0/I = f(C_{\text{cation}}^2)$ linear dependency following the Stern–Volmer method.

values. The goal at this stage of our research work was to provide initial information on the influence of the type of linkage between Fc and sumanene on Cs^+ binding exhibited by the conjugates considering the relative differences between the binding parameters. All the conjugates exhibited high association constant values in terms of Cs^+ binding (with the K_a value in the range of 10^4–10^5) together with low limits of detection (LOD = 1.8–7.0 × 10^{-5} M). A direct comparison between the K_a values leads to the following conclusions: (1) the probes comprised of the *p*-phenylenediamine-type linkage showed *ca.* 3- and 1.5-fold higher K_a than the respective conjugates without the above-mentioned spacer (**3** *vs.* **8** and **4** *vs.* **9**), (2) the samples containing the CH_2NH-type linkage exhibited *ca.* 10-fold higher K_a than the respective conjugates bearing the imine-type moiety (**3** *vs.* **4**, **8** *vs.* **9**), and (3) the di-sumanenyl derivative **5** showed *ca.* 2-fold higher K_a than the respective mono-sumanenyl derivative **4**.

^1H NMR titration provided further insight into the interaction pattern. The experiments were performed for the representative compounds **3** (CH_2NH-type linkage) and **4** (imine-type spacer). A significant downfield shift for the benzylic *endo* protons of the sumanene moiety in these compounds was observed after the addition of further portions of Cs^+.[27,28] In contrast, the corresponding *exo* protons did not show any significant change in their chemical shifts. This observation confirmed that the concave face of the sumanene moiety is strongly involved in the interaction with Cs^+. The sumanene–Cs^+ interaction (compounds **3–5** and **8–9**) could also be tracked by CV, as (1) the lowering of oxidation current intensity and (2) the presence of a new peak at a lower potential ($E^{\text{ox}}_{\text{max}}$ = 0.235–0.075 V) were observed upon the addition of excess Cs^+.[20] Such trends have been previously demonstrated to be the characteristic features of the ion sensing phenomenon.[5] This trial also showed the potential application of the obtained ferrocene–sumanene conjugates in Cs^+ recognition using the electrochemical methods.

To study the significance of the sumanene moiety in compounds **3–5** and **8–9** in their Cs^+ recognition ability, a ferrocene–naphthalene conjugate (**10**) was synthesized as a reference for the fragment of the ferrocene–sumanene conjugate **3**, with the difference in the structural moiety (sumanene (**3**) *vs.* naphthalene (**10**)) (Fig. 4a).[11] The ^1H NMR titration pattern[27] as well as the emission spectrum of compound **10** (Fig. 4b)

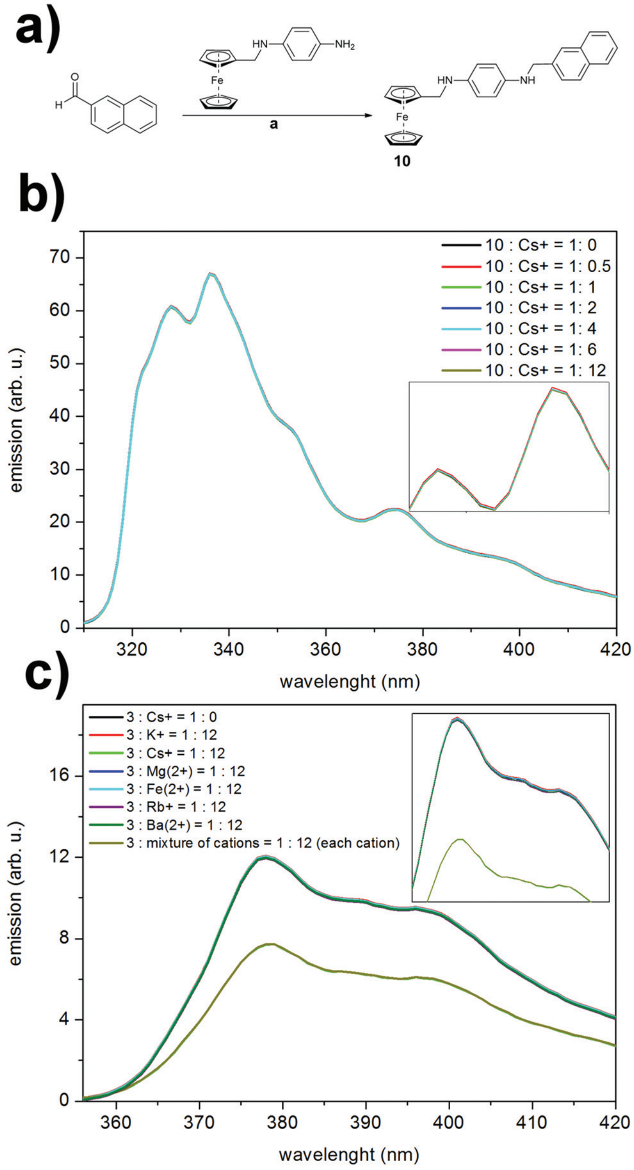

Fig. 4 (a) Synthesis of ferrocene–naphthalene conjugate **10** (conditions a: *N*-(ferrocenylmethyl)benzene-1,4-diamine 100 mol%, 2-naphthaldehyde 100 mol%, formic acid (cat.), MeOH, 27 °C, 27 h, then $NaBH_4$ 300 mol%, 27 °C, 3 h, 67% yield.); (b) caesium (Cs^+) binding studies with compound **10** using the fluorescence spectra titration method (excitation wavelength: 280 nm); (c) different cation binding studies with compound **3** using the fluorescence spectra titration method (excitation wavelength: 280 nm).[30]

remained unchanged after the addition of further portions of Cs^+.[29] This feature clearly showed that the presence of the sumanene moiety in compounds **3**–**5** and **8**–**9** was essential for their Cs^+ binding ability. The interaction of the representative ferrocene–sumanene conjugate **3** with other cations, namely K^+, Mg^{2+}, Fe^{2+}, Rb^+ and Ba^{2+}, was also studied (fluorescence spectroscopy assay; Fig. 4c). No change in the emission intensity of compound **3** was observed after the addition of other cations. This is especially important for trials with Rb^+ and Ba^{2+}, as no interaction between these metal cations and the studied Fc-sumanene probes was observed which means that the metal ions of similar radii do not interfere in Cs^+ recognition. These results further confirmed the selective interaction of the ferrocene–sumanene conjugate with Cs^+, due to the perfect match of Cs^+ with the sumanene's concave site. Our study also included the comparison between the emission intensity of (i) the sample containing compound **3** with the excess of Cs^+ and (ii) the sample containing compound **3** with the excess of the mixture of cations (12 eq. each) (Fig. 4c). No significant difference between these samples was observed. This finding provided the evidence that the designed ferrocene–sumanene conjugates can be used for the recognition of Cs^+ in ion-rich samples.

In conclusion, our work revealed that the sumanene-based ferrocene-templated conjugates can be applied as selective and efficient caesium cation (Cs^+) recognition materials. The novelty of this work included the evidence that the site-selective 'cation–π interaction' with the inclusion of the sumanene's concave face enabled the selective binding of Cs^+. The interactions can be tracked both spectroscopically (fluorescence spectra titration and ^1H NMR titration) and electrochemically (cyclic voltammetry). Taking into account high association constant values exhibited by all of the conjugates (in the range of 10^4–10^5) and low limits of detection (LOD = $1.8–7.0 \times 10^{-5}$ M), our work sheds light on the unexplored applications of compounds bearing a buckybowl motif and the cation–π interaction phenomenon. This work presents a new application of the 'cation–π interaction' phenomenon in the development of binding sites for the design of selective receptors of metal ions.

Conflicts of interest

There are no conflicts to declare.

Acknowledgements

This study was supported by a Grant-in-Aid for Scientific Research on Innovative Area 'π System Figuration' from the MEXT (No. JP26102002). A. K. acknowledges the National Science Centre (Poland) for the ETIUDA scholarship (No. 2018/28/T/ST5/00018) and the Foundation for Polish Science (Poland) for the START scholarship. The authors appreciate the experiments performed by Dr Fong Jiao Hong, Univ. Malaya toward aminosumanene synthesis.

Notes and references

1 (*a*) G. Brumfiel, *Nature*, 2011, **472**, 146–147; (*b*) T. J. Yasunari, A. Stohl, R. S. Hayano, J. F. Burkhart, S. Eckhardt and T. Yasunari, *Proc. Natl. Acad. Sci. U. S. A.*, 2011, **108**, 19530–19534; (*c*) Y. Masumoto, Y. Miyazawa, D. Tsumune, T. Tsubono, T. Kobayashi, H. Kawamura, C. Estournel, P. Marsaleix, L. Lanerolle, A. Mehra and Z. D. Garraffo, *Elements*, 2012, **8**, 207–212.

2 (*a*) A. Depauw, N. Kumar, M.-H. Ha-Thi and I. Leray, *J. Phys. Chem. A*, 2015, **119**, 6065–6073; (*b*) H.-F. Ji, R. Dabestani, G. M. Brown and R. A. Sachleben, *Chem. Commun.*, 2000, 833–834; (*c*) J. S. Kim, H. Suh, J. K. Kimc and M. H. Cho, *J. Chem. Soc., Perkin Trans. 1*, 1998, 2307–2312; (*d*) V. Souchon, I. Leray and B. Valeur, *Chem. Commun.*, 2006, 4224–4226; (*e*) S. K. Kim, G. I. Vargas-Zuniga, B. P. Hay, N. J. Young, L. H. Delmau, C. Masselin, C.-H. Lee, J. S. Kim, V. M. Lynch, B. A. Moyer and J. L. Sessler, *J. Am. Chem. Soc.*, 2012, **134**, 1782–1792.

3 (*a*) A. Scozzari, Electrochemical Sensing Methods: A Brief Review, in *Algal Toxins: Nature, Occurrence, Effect and Detection*, ed. V. Evangelista, L. Barsanti, A. M. Frassanito, V. Passarelli and P. Gualtieri, 2008; (*b*) A. M. Ashrafi, Z. Koudelkova, E. Sedlackova, L. Richtera and V. Adam, *J. Electrochem. Soc.*, 2018, **165**, B824–B834; (*c*) B. Silwana, C. Van Der Horst, E. Iwuoha and V. Somerset, *J. Environ. Sci. Health, Part A: Toxic/Hazard. Subst. Environ. Eng.*, 2016, **51**, 1233–1247.

4 (*a*) D. Astruc, *Eur. J. Inorg. Chem.*, 2017, 6–29; (*b*) O. B. Sutcliffe, A. Chesney and M. R. Bryce, *J. Organomet. Chem.*, 2001, **637–639**, 134–138; (*c*) F. Zapata, A. Caballero, A. Tárraga and P. Molina, *J. Org. Chem.*, 2010, **75**, 162–169.

5 See for example: (*a*) T. Romero, A. Caballero, A. Tarraga and P. Molina, *Org. Lett.*, 2009, **11**, 3466–3469; (*b*) H. Huang, Z. Xin, L. Yuan, B.-Y. Wang and Q.-Y. Cao, *Inorg. Chim. Acta*, 2018, **483**, 425–430.

6 (*a*) S. Higashibayashi and H. Sakurai, *Chem. Lett.*, 2011, **40**, 122–128; (*b*) T. Amaya and T. Hirao, *Chem. Rec.*, 2015, **15**, 310–321; (*c*) M. Saito, H. Shinokubo and H. Sakurai, *Mater. Chem. Front.*, 2018, **2**, 635–661.

7 H. Sakurai, T. Daiko and T. Hirao, *Science*, 2003, **301**, 1878.

8 (*a*) Y. Shoji, T. Kajitani, F. Ishiwari, Q. Ding, H. Sato, H. Anetai, T. Akutagawa, H. Sakurai and T. Fukushima, *Chem. Sci.*, 2017, **8**, 8405–8410; (*b*) I. Hisaki, H. Toda, H. Sato, N. Tohnai and H. Sakurai, *Angew. Chem., Int. Ed.*, 2017, **56**, 15294–15298.

9 B. Topolinski, B. M. Schmidt, S. Higashibayashi, H. Sakurai and D. Lentz, *Dalton Trans.*, 2013, **42**, 13809–13812.

10 S. N. Spisak, Z. Wei, A. Y. Rogachev, T. Amaya, T. Hirao and M. A. Petrukhina, *Angew. Chem., Int. Ed.*, 2017, **56**, 2582–2587.

11 For experimental details, see the Experimental section in the ESI.† The reaction scheme dealing with the synthesis of ferrocene derivatives used is also presented therein (Scheme S1).†

12 B. B. Shrestha, S. Karanjit, G. Panda, S. Higashibayashi and H. Sakurai, *Chem. Lett.*, 2013, **42**, 386–388.

13 For NMR spectra, see section S2 in the ESI.†

14 ^{1}H–^{1}H COSY NMR spectra enabled (1) the confirmation of the chemical shifts of the benzylic *endo* and benzylic *exo* protons coming from the sumanene moiety, (2) the confirmation of the signal overlapping for compound **3** (benzylic *endo* + N**H**–CH$_2$-sumanene), and (3) the assignment of the respective N**H** and C**H$_2$** protons. The ^{1}H–^{1}H TOCSY NMR spectrum of compound **3** enabled the confirmation of the inclusion of the C**H$_2$**-sumanene and Ar–**H** (sumanene) protons in the same spin system, and thus the multiplicity of this signal was supported. See the discussion and the 2-D NMR spectra in section S2 in the ESI.†

15 For IR spectra, see section S3 in the ESI.†

16 For UV-Vis spectra, see section S4 in the ESI.† In addition, UV-Vis spectra excluded experimentally any possible charge transfer phenomenon between ferrocene and sumanene moieties. Therefore, the sumanene moiety remains neutral throughout further binding with Cs$^+$.

17 The absorption maximum coming from the imine moiety for compounds **4**, **5**, and **9** overlapped with the Fc's absorption maximum (*ca.* 390–360 nm).

18 For the discussion on the dependency of the type of substituent on the Fc's oxidation/reduction peak position, see for example: N. G. Tsierkezos, *J. Solution Chem.*, 2007, **36**, 289–302.

19 In the reference, the Fc oxidation peak was at $E_{1/2}^{\mathrm{ox}} = 0.298$ V.

20 See section S8 in the ESI† for cyclic voltammograms.

21 See section S5 in the ESI† for the fluorescence titration spectra of other ferrocene–sumanene conjugates (**4–5** and **8–9**). The UV-Vis spectra titration method was also applied for tracking the binding phenomenon, however this technique was found to be not as sensitive as the fluorescence spectra titration method (see the plots for representative compound **3** in Fig. S43, ESI†). Thus, further analyses and calculations were based on the fluorescence spectra titration experiments.

22 Due to the solubility of the studied compounds (CsCl – soluble in MeOH, not soluble in halogenated solvents; compounds **3–5** and **8–9** – soluble in halogenated solvents, not soluble in MeOH), the binding studies were performed in a mixed solvent system: MeOH : CHCl$_3$ = 1/1 v/v.

23 See for example: (*a*) P. Kaur, H. Kaur and K. Singh, *RSC Adv.*, 2013, **3**, 64–67; (*b*) P. N. Borase, P. B. Thale and G. S. Shankarling, *Dyes Pigm.*, 2016, **134**, 276–284; (*c*) T. Nesakumar, J. I. Edisona, R. Atchudan, J.-J. Shim, S. Kalimuthu, B.-C. Ahn and Y. R. Lee, *J. Photochem. Photobiol., B*, 2016, **158**, 235–242.

24 For Job's plots, see section S6 in the ESI.†

25 The studied Cs$^+$ recognition phenomenon using the Fc–sumanene conjugates did not utilize the ligation of the metal ion at the heteroatom. Theoretical evidence for the observed cation–π interaction with buckybowls was previously provided, see: (*a*) U. D. Priyakumar and G. N. Sastry, *Tetrahedron Lett.*, 2003, **44**, 6043–6046; (*b*) U. D. Priyakumar, M. G. P. Krishna and G. N. Sastry, *Tetrahedron Lett.*, 2004, **60**, 3037–3043; (*c*) D. Vijay, H. Sakurai, V. Subramanian and G. N. Sastry, *Phys. Chem. Chem. Phys.*, 2012, **14**, 3057–3065; (*d*) M. Rellán-Piñeiro, J. Rodríguez-Otero, E. M. Cabaleiro-Lago and D. Josa, *J. Mol. Model.*, 2013, **19**, 2049–2055.

26 For the basis of this method, see for example: A. M. Pyle, J. P. Rehmann, R. Meshoyrer, C. V. Kumar, N. J. Turro

and J. K. Barton, *J. Am. Chem. Soc.*, 1989, **111**, 3051–3058. The details of calculations are given in the ESI, section S9.†

27 See section S7 in the ESI† for ^{1}H NMR titration spectra.

28 Studies performed in a mixed solvent system: $CD_3OD : CDCl_3$ = 1/1 v/v.

29 Despite the good solubility of compound **10** in MeOH, the binding studies were performed in a mixed solvent system ($MeOH : CHCl_3$ = 1/1 v/v), in order to provide a direct comparison with the results obtained for the sumanene–ferrocene conjugates **3–5** and **8–9**.

30 See section S5 in the ESI for fluorescence titration spectra.†